Influence of surface states on quantum and transport lifetimes in high-quality undoped heterostructures

D. Q. Wang,[1] J. C. H. Chen,[1] O. Klochan,[1] K. Das Gupta,[2,*] D. Reuter,[3,†] A. D. Wieck,[3]
D. A. Ritchie,[2] and A. R. Hamilton[1]

[1]*School of Physics, University of New South Wales, Sydney NSW 2052, Australia*
[2]*Cavendish Laboratory, J. J. Thomson Avenue, Cambridge, CB3 OHE, United Kingdom*
[3]*Angewandte Festkörperphysik, Ruhr-Universität Bochum, D-44780 Bochum, Germany*

(Received 3 April 2013; published 23 May 2013)

We present a comparison between experimental and theoretical values of transport τ_t and quantum τ_q scattering lifetimes in high-quality undoped $Al_{0.34}Ga_{0.66}As/GaAs$ heterostructures. We obtain excellent agreement between the experimental and modeled scattering times using three scattering processes: background impurity, interface roughness, and remote ionized impurity scattering from surface states. We show that despite the high mobility ($\mu_{peak} = 5.6 \times 10^6$ cm^2 V^{-1} s^{-1}), the quantum lifetime τ_q is significantly reduced by small-angle scattering from remote surface charge. We further show that in shallow devices scattering from surface charges will be a limiting factor for both transport and quantum lifetimes.

DOI: 10.1103/PhysRevB.87.195313 PACS number(s): 73.43.Qt, 73.40.Kp, 68.35.Ct, 81.05.Ea

I. INTRODUCTION

For many years, modulation-doped AlGaAs/GaAs heterostructures have been the center of research on low-dimensional systems. While extremely high mobility two-dimensional (2D) systems[1–3] have been realized in modulation-doped heterostructures,[4,5] remote ionized impurities, which can act as an additional source of disorder causing both Coulomb scattering and long-range fluctuation of the potential landscape, are introduced to the system ineluctably.[6–8] Due to these ionized impurities, the closer the 2D systems are brought to the surface, the more affected electron transport is.[9] Therefore, although it is possible to attain high electron mobility in deep 2D electron systems, achieving similar mobility in shallower 2D systems which are desirable for nanostructures with fine lithographic configurations remains problematic.

Recently undoped heterostructures have drawn attention due to some obvious advantages over modulation-doped heterostructures.[6–8,10–12] Owing to the removal of intentional doping, undoped heterostructures are expected to have fewer ionized impurities, the presence of which is the predominant factor limiting the 2D transport performance of shallow modulation-doped heterostructures.[9] Nanostructures fabricated using shallow undoped AlGaAs/GaAs heterostructures have been shown to have much improved electron mobility[13] compared to similarly shallow modulation-doped ones. However, there still exists one possible drawback for metal-gated undoped heterostructures: Unavoidable surface charge may affect the carriers in a manner similar to remote ionized impurity scattering, adding unwanted disorder to undoped devices. Although it has been shown that surface charge reduces the 2DEG mobility of very shallow systems,[14] there is little understanding of its effects on 2DEGs of deep undoped heterostructures, or on the stability of devices based on shallow 2D systems. In this paper we present both experimental and theoretical analysis of undoped heterostructures showing that even though the carrier mobility is not affected by surface states when the 2DEG is deep, the electron quantum lifetime τ_q is significantly reduced by surface charge in high-quality undoped heterostructures.

II. EXPERIMENTAL RESULTS

A. Sample and experimental setup

The undoped device used in the experiment is a single heterojunction Hall bar fabricated on wafer B13520, which has a 17 nm GaAs cap followed by 300 nm undoped $Al_{0.34}Ga_{0.66}As$ and then a 1 μm GaAs buffer. Polyimide is used as the insulator between the ohmics and the top-gate metal. Detailed fabrication methods and schematics of the device can be found in Ref. 15. Magnetotransport measurements were performed in a dilution fridge with a constant excitation voltage of 100 μV using standard lock-in techniques. The base temperature of the dilution fridge was 25 mK and the base electron temperature was 80 mK determined from measurements of variable range hopping[16] in a similar sample with the same measurement setup. By changing the voltage applied to the top gate, we varied the 2DEG density over an order of magnitude from 1.3×10^{10} to 1.5×10^{11} cm^{-2} as shown in Fig. 1(a). The 2DEG density is linear with the top-gate bias and its gradient is determined by the separation between the top gate and the 2DEG. The 2DEG mobility is plotted as a function of density in Fig. 1(b). The 2DEG mobility increases monotonically with the carrier density and reaches 5.6×10^6 cm^2/V s at $n_s = 1.5 \times 10^{11}$ cm^{-2}, the highest density measured at $V_{TG} = 7$ V. Top-gate biases larger than 7 V were not applied to avoid breakdown of the polyimide gate dielectric. For $V_{TG} \leqslant 7$ V, the gate leakage was below the measurement resolution of 10 pA.

B. Measurements of lifetimes from Shubnikov–de Haas oscillations

Figure 2 shows the low-field Shubnikov–de Haas (SdH) oscillations and Hall resistance for three different densities. The SdH oscillations show clear zeros and no parallel conduction. The amplitude of the SdH oscillations can be

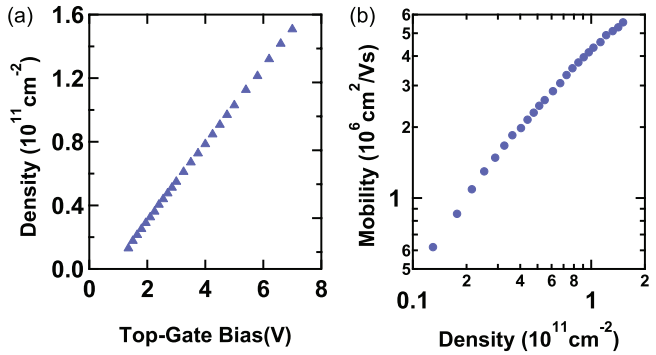

FIG. 1. (Color online) Device characterization: (a) 2DEG density as a function of applied top-gate bias obtained from the low-field Hall resistance. (b) 2DEG mobility as a function of density.

written as[17]

$$\Delta R_{xx} = 4R_0X(T)\exp(-\pi/\omega_c\tau_q), \tag{1}$$

where R_0 is the zero-field resistance, ω_c is the cyclotron frequency, and $X(T)$ is a thermal damping factor given by

$$X(T) = (2\pi^2kT/\hbar\omega_c)/\sinh(2\pi^2kT/\hbar\omega_c). \tag{2}$$

The quantum lifetime τ_q can be obtained from a Dingle plot of the logarithm of $\Delta R_{xx}/R_0X(T)$ versus $1/B$. In a "good" Dingle plot, the intercept at $1/B = 0$ is 4 and the slope of the resultant straight line gives τ_q.[17] Figure 3 shows the Dingle plots used to extract τ_q. The data are well described by straight lines with a fixed intercept of 4, leaving the slope as the only fitting parameter. All Dingle plots show excellent agreement between the experimental data and fitting lines, which suggests that reliable values of τ_q have been obtained.

The extracted τ_q is then plotted as a function of density, together with the transport scattering lifetime τ_t obtained from the 2DEG mobility, as shown by the triangles in Fig. 4. Solid down-pointing triangles show the measured τ_q with a fixed $1/B = 0$ intercept of 4 for Dingle plots while the open triangles show the τ_q obtained with the intercept used as a second fitting parameter. The two fitting methods give only a 15% difference in τ_q on average. Both τ_q and τ_t

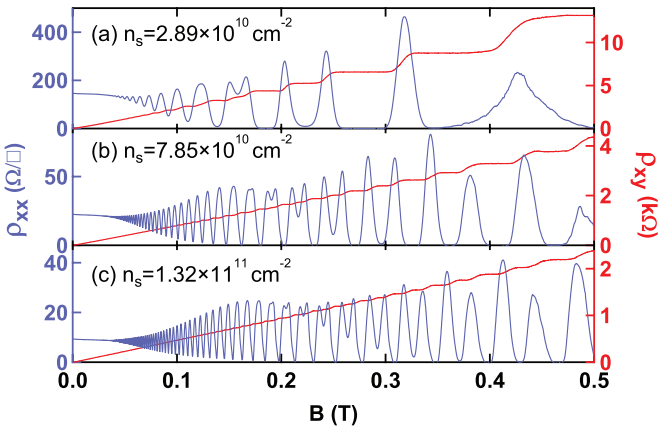

FIG. 2. (Color online) Shubnikov–de Haas oscillations and Hall resistance for three different 2DEG densities.

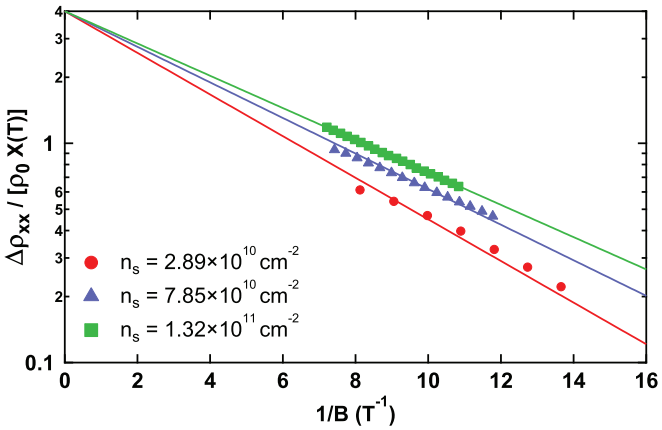

FIG. 3. (Color online) Dingle plots for three different densities corresponding to the ρ_{xx} data shown in Fig. 2, using an electron temperature of 80 mK from variable range hopping measurements[16] on a similar sample with the same experimental setup. It is worth noting that Dingle plots are insensitive to the carrier temperature used—a 10 mK difference in the temperature only results in a 1% change in τ_q with our fitting method where the $1/B = 0$ intercept is fixed at 4. Moreover, if the intercept is left as a fitting parameter, the thermal correction term $X(T)$ which contains the temperature only affects the intercept of Dingle plots, but does nothing to the slope or the value of τ_q.

increase as the density increases, while τ_t increases faster with n_s than τ_q. To understand the role of different scattering mechanisms we compared our experimental results with numerical calculations.

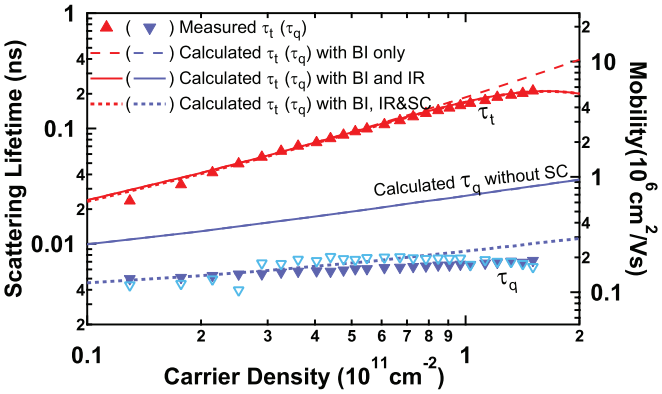

FIG. 4. (Color online) Experimental and theoretical scattering lifetimes plotted as a function of density with the right axis showing corresponding mobility calculated using $\mu_{q,t} = e\tau_{q,t}/m$. The symbols show the measured τ_t and τ_q. Dashed lines show τ_t and τ_q calculated with background impurity (BI) scattering only. Solid lines show τ_t and τ_q calculated with both BI and interface roughness (IR) scattering. Dotted lines show τ_t and τ_q calculated with BI, IR, and surface charge (SC) scattering. The calculated τ_t including SC scattering (dotted line) is very close to the values of τ_t calculated with BI and IR scattering only (solid line) and can hardly be distinguished. The calculated τ_q with (solid line) or without (dashed line) IR scattering lie on top of each other as the addition of IR scattering does not alter τ_q.

III. COMPARISON WITH THEORY AND DISCUSSIONS

At $T = 0$ the transport scattering lifetime τ_t can be calculated as[18]

$$\frac{1}{\tau_t} = \frac{m^*}{\pi\hbar^3 k_F^2}\int_0^{2k_F} \frac{|\,U(q)\,|^2}{\epsilon(q)^2}\frac{q^2}{\sqrt{4k_F^2 - q^2}}dq, \tag{3}$$

where $|U(q)|^2$ is the scattering potential and $\epsilon(q)$ is the screening function. The transport lifetime τ_t shows a different density dependence for different scattering mechanisms, which can be used to identify the various scattering processes in the system. The dominant scattering mechanism in deep undoped heterostructures is Coulomb scattering from background impurities,[14,18] for which $|U(q)|^2$ is given by[18]

$$|U(q)|^2_{\rm BG} = \frac{1}{2q}\left(\frac{e^2}{2\epsilon\epsilon_0 q}\right)^2 [N_{b_{\rm Al_{0.34}Ga_{0.66}As}} F_{\rm Al_{0.34}Ga_{0.66}As}(q) + N_{b_{\rm GaAs}} F_{\rm GaAs}(q)], \tag{4}$$

where $F(q)$ is the form factor. The experimental τ_t is well described with background impurities as the sole scattering mechanism, as shown by the dashed line in Fig. 4 with $N_{b_{\rm AlGaAs}} = 1.65 \times 10^{14}\ {\rm cm}^{-3}$ and $N_{b_{\rm GaAs}} = 5.5 \times 10^{13}\ {\rm cm}^{-3}$. The higher impurity density in AlGaAs is consistent with previous studies.[14,15,18] The only discrepancy between the calculation and measured mobility occurs at densities above $8 \times 10^{10}\ {\rm cm}^{-2}$, when interface roughness scattering starts to take over and limit the mobility. Interface roughness scattering can be modeled using the following scattering potential:

$$|U(q)|^2_{\rm IR} = \pi\Lambda^2\Delta^2\left(\frac{n_{2D}e^2}{2\epsilon\epsilon_0}\right)^2 \exp^{-\frac{1}{4}\Lambda^2 q^2}, \tag{5}$$

where we use $\Delta = 2$ Å as the amplitude and $\Lambda = 4$ nm as the correlation length of the roughness. Including interface roughness scattering gives excellent agreement between experimental τ_t and the calculations over the whole density range as shown by the solid line in Fig. 4.

The single-particle lifetime τ_q, which counts both small-angle and large-angle scattering processes and differs from τ_t by the weighting factor $1 - \cos(\theta)$, is more complex than calculating τ_t since the first order approximation

$$\frac{1}{\tau_q} = \frac{2m^*}{\pi\hbar^3}\int_0^{2k_F} \frac{|U(q)|^2}{\epsilon(q)^2}\frac{1}{\sqrt{4k_F^2 - q^2}}dq \tag{6}$$

has a logarithmic divergence.[19] To solve this problem we used multiple-scattering theory[19] to calculate the renormalized τ_q following the method in Ref. 18. The calculated τ_q is plotted as the solid line in Fig. 4. Surprisingly, the values of τ_q calculated with the same background impurity density and interface roughness used to fit the τ_t data are more than double the values of the measured τ_q. This discrepancy can be explained by introducing another scattering process—scattering from remote surface charges. Since polyimide is used as the insulator between the top gate and the ohmic contacts,[15] charge can be trapped at the interface between the polyimide and the GaAs cap layer.[20] This surface charge acts like remote ionized impurities, scattering electrons in the 2DEG.[14] To model the scattering caused by this extra disorder, we considered a sheet of charged impurities with an areal density of N_{sc} at a distance d from the 2DEG, for which the scattering potential is given by

$$|U(q)|^2_{\rm SURF} = N_{\rm sc}\left(\frac{e^2}{2\epsilon\epsilon_0}\right)^2 \exp(-2qd)F(q). \tag{7}$$

With $N_{\rm sc} = 0.9 \times 10^{11}\ {\rm cm}^{-2}$ and $d = 300$ nm, we greatly improved the fitting between theoretical and experimental values of τ_q as shown by the dotted line in Fig. 4. It is important to note that adding this extra disorder makes little difference to the calculated values of τ_t. This is expected as the surface charge is far from the 2DEG, and only causes small-angle scattering events which hardly affect τ_t. However, τ_q is sensitive to all scattering events, so is strongly affected by the surface charge.

We note that although the fitting of τ_q is significantly improved by including surface charge scattering, there still exists a small discrepancy between the theoretical and experimental τ_q at densities above $7 \times 10^{10}\ {\rm cm}^{-2}$ which cannot be explained using our model. It is tempting to ascribe this discrepancy to interface roughness scattering, but unlike τ_t including interface roughness scattering does not improve the agreement between experiment and modeling in the high-density regime. This is because the quantum scattering rate from interface roughness is negligible compared to that from charged impurities (interface roughness scattering only has a very small effect on τ_t, yet since it is a large angle it will affect both τ_t and τ_q equally).

IV. PREDICTIONS AND CONCLUSIONS

We now investigate how this unavoidable surface charge will affect shallow 2D systems. We have calculated the single particle and transport lifetimes as a function of the depth of the 2DEG at a density of $1 \times 10^{11}\ {\rm cm}^{-2}$ using the same model and impurity densities as in Fig. 4. From the calculation result plotted in Fig. 5, we can see that at $n_s = 1 \times 10^{11}\ {\rm cm}^{-2}$ the transport lifetime τ_t remains insensitive to small-angle

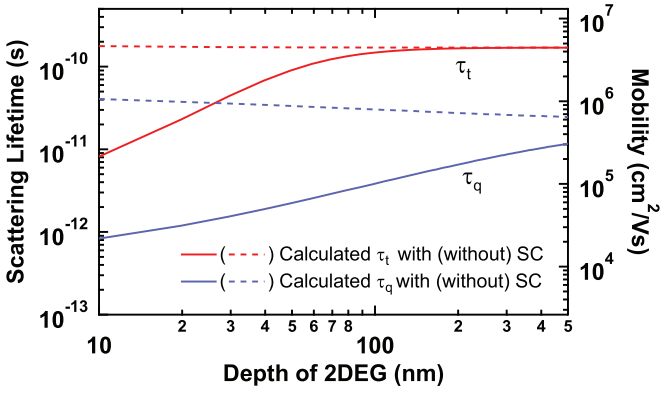

FIG. 5. (Color online) Calculated scattering lifetimes as a function of the depth of the 2DEG at $n_s = 10^{11}\ {\rm cm}^{-2}$, evaluated using three scattering mechanisms: background impurity scattering, interface roughness scattering, and remote ionized impurity scattering due to surface charge. Dashed lines are the scattering lifetimes calculated with background impurity and interface roughness scattering, while solid lines are the values calculated with scattering from surface states also included. All parameters used are the same as in Fig. 4.

scattering caused by surface states if the 2DEG is deeper than 60 nm, whereas the quantum lifetime τ_q is strongly affected at similar or even greater depths. For shallow systems where the 2DEG depth is usually less than 60 nm, both τ_t and τ_q are affected by surface states, although the reduction in τ_t stays lower than that of τ_q. Moreover, the calculation also shows that even if all background impurities could be removed, ultrahigh electron mobilities can only be achieved in insulated gate devices if the 2DEG is deeper than 200 nm. To further explore the effects of surface states in shallow systems, we have also repeated the calculation in Fig. 5 for different carrier densities. The calculations show that as the 2DEG density increases, the depth at which the 2DEG mobility starts to be affected by surface states gets shallower. This result can be explained by the matrix element of surface charge scattering. As shown by Eq. (7), the term $\exp(-2qd)$ is always less than 1 since both the wave vector q and the distance d are positive. Therefore, the greater the product qd is, the less electrons are scattered by surface charge. Since the mobility is strongly affected by the $q \simeq 2k_F$ backscattering process, if the depth of the 2DEG d is decreased, the density must be increased to increase k_F to keep the same amount of surface charge scattering. Accordingly, the shallower the 2DEG is, the higher the carrier density must be to attain high mobility. Our results also show that even though high mobility can be achieved in undoped shallow wafers at a large carrier density,[12] scattering from surface charge will affect device performance through the reduction of τ_q. As a result, all quantum lifetime or phase related measurements based on insulated-gate heterostructures, such as the Aharonov-Bohm effect[21] and the observation of the $\nu = 5/2$ fractional quantum Hall effect (FQHE) states,[12,22] will be significantly influenced even though the electron mobility can be high and modulation doping has been removed. In addition, it can be hard to make high-mobility nanostructures on very shallow undoped wafers in the presence of surface charge scattering. A possible way to eliminate the effects of surface charge is by using a semiconductor-insulator-semiconductor field-effect transistor (SISFET) structure, in which a degenerately doped cap acts as the top gate[7,23] and screens the 2DEG from surface charge, allowing mobilies over 10^7 cm^2/V s. However, while extremely useful for large area 2D devices, the SISFET structure has drawbacks for making nanostructures. To define small features the 2DEG should be shallow, but in the SISFET it is hard to form ohmic contacts to a shallow 2DEG without shorting to the doped cap. Second, the degenerately doped $n+$ or $p+$ GaAs cap used in the SISFET is not suitable for extremely small gate patterns. This is because the gates are defined by etching the cap, and surface state pinning means that gates narrower than $\sim$70 nm are no longer metallic.[24]

In conclusion, we have measured the transport and quantum lifetimes of an induced 2DEG at a single $Al_{0.34}Ga_{0.66}As$/GaAs heterojunction and compared the results with theoretical calculations. From the comparison we have detected the existence of surface charge and demonstrated its effects on the scattering lifetimes for deep undoped heterostructures. We found that the quantum lifetime τ_q is significantly reduced by surface charge even though the 2DEG is 300 nm deep and its transport mobility is unaffected. These findings will be important for the development of high quality induced nanostructures.

ACKNOWLEDGMENTS

We thank F. Sfigakis and A. Croxall for helpful discussions. This work was funded by the Australian Research Council through the DP scheme, and by the Australian Government under the Australia-India Strategic Research Fund—a component of the Australian Scholarships initiative.

*Now at Department of Physics, IIT Bombay, Mumbai 400076, India.
†Now at Arbeitsgruppe fur optoelektronische Materialien und Bauelemente, Universität Paderborn, 33098 Paderborn, Germany.

[1] L. N. Pfeiffer, K. W. West, H. L. Störmer, and K. W. Baldwin, Appl. Phys. Lett. **55**, 1888 (1989).
[2] W. Pan, J. S. Xia, H. L. Störmer, D. C. Tsui, C. Vicente, E. D. Adams, N. S. Sullivan, L. N. Pfeiffer, K. W. Baldwin, and K. W. West, Phys. Rev. B **77**, 075307 (2008).
[3] V. Umansky, M. Heiblum, Y. Levinson, J. Smet, J. Nübler, and M. Dolev, J. Cryst. Growth **311**, 1658 (2009).
[4] R. Dingle, H. L. Störmer, A. C. Gossard, and W. Wiegmann, Appl. Phys. Lett. **33**, 665 (1978).
[5] T. Mimura, S. Hiyamizu, T. Fujii, and K. Nanbu, Jpn. J. Appl. Phys. **19**, L225 (1980).
[6] B. E. Kane, L. N. Pfeiffer, K. W. West, and C. K. Harnett, Appl. Phys. Lett. **63**, 2132 (1993).
[7] B. E. Kane, L. N. Pfeiffer, and K. W. West, Appl. Phys. Lett. **67**, 1262 (1995).
[8] F. Sfigakis, K. Das Gupta, S. Sarkozy, I. Farrer, D. A. Ritchie, M. Pepper, and G. A. C. Jones, Physica E **42**, 1200 (2010).
[9] D. Laroche, S. Das Sarma, G. Gervais, M. P. Lilly, and J. L. Reno, Appl. Phys. Lett. **96**, 162112 (2010).
[10] A. M. See, I. Pilgrim, B. C. Scannell, R. D. Montgomery, O. Klochan, A. M. Burke, M. Aagesen, P. E. Lindelof, I. Farrer, D. A. Ritchie, R. P. Taylor, A. R. Hamilton, and A. P. Micolich, Phys. Rev. Lett. **108**, 196807 (2012).
[11] W. R. Clarke, C. E. Yasin, A. R. Hamilton, A. P. Micolich, M. Y. Simmons, K. Muraki, Y. Hirayama, M. Pepper, and D. A. Ritchie, Nat. Phys. **4**, 55 (2008).
[12] W. Pan, N. Masuhara, N. S. Sullivan, K. W. Baldwin, K. W. West, L. N. Pfeiffer, and D. C. Tsui, Phys. Rev. Lett. **106**, 206806 (2011).
[13] W. Y. Mak, F. Sgakis, K. Das Gupta, O. Klochan, H. E. Beere, I. Farrer, J. P. Griths, G. A. C. Jones, A. R. Hamilton, and D. A. Ritchie, Appl. Phys. Lett. **102**, 103507 (2013).
[14] W. Y. Mak, K. Das Gupta, H. E. Beere, I. Farrer, F. Sfigakis, and D. A. Ritchie, Appl. Phys. Lett. **97**, 242107 (2010).
[15] J. C. H. Chen, D. Q. Wang, O. Klochan, A. P. Micolich, K. Das Gupta, F. Sfigakis, D. A. Ritchie, D. Reuter, A. D. Wieck, and A. R. Hamilton, Appl. Phys. Lett. **100**, 052101 (2012).
[16] N. F. Mott, Philos. Mag. **19**, 835 (1969).
[17] P. T. Coleridge, Phys. Rev. B **44**, 3793 (1991).
[18] S. J. MacLeod, K. Chan, T. P. Martin, A. R. Hamilton, A. See, A. P. Micolich, M. Aagesen, and P. E. Lindelof, Phys. Rev. B **80**, 035310 (2009).

[19] A. Gold, Phys. Rev. B **38**, 10798 (1988).
[20] J. H. Davies and I. A. Larkin, Phys. Rev. B **49**, 4800 (1994).
[21] G. Timp, A. M. Chang, J. E. Cunningham, T. Y. Chang, P. Mankiewich, R. Behringer, and R. E. Howard, Phys. Rev. Lett **58**, 2814 (1987).
[22] H. C. Choi, W. Kang, S. Das Sarma, L. N. Pfeiffer, and K. W. West, Phys. Rev. B **77**, 081301 (2008).
[23] W. R. Clarke, A. P. Micolich, A. R. Hamilton, K. Muraki, M. Y. Simmons, and Y. Hirayama, J. Appl. Phys. **99**, 023707 (2006).
[24] A. M. See, O. Klochan, A. R. Hamilton, A. P. Micolich, M. Aagesen, and P. E. Lindelof, Appl. Phys. Lett. **96**, 112104 (2010).